Deformational Properties of Filled Rubber Under Quasistatic Loading

Klara Aniskevich, Olesja Starkova, Andrey Aniskevich

Institute of Polymer Mechanics, Aizkraukles 23, Riga, Latvia

Received 9 November 2009; accepted 22 March 2011
DOI 10.1002/app.34557
Published online 19 August 2011 in Wiley Online Library (wileyonlinelibrary.com).

ABSTRACT: To go ahead in understanding the nature of rubber reinforcement and evaluate the kinetics of filler clusters destruction during stretching of filled rubber, the styrene-butadiene rubber both unfilled and filled with various contents of silica particles with and without surface treatment was tested under quasistatic loading up to failure. The Klueppel–Schramm model was used for description of strain softening, evaluation of both the rubber and filler network parameters as the functions of the filler volume content. It was found that an elastic modulus as a function of filler volume content follows Guth–Gold equation, confirming the hydrodynamic nature of the rubber reinforcement; the effectiveness factor depends on filler surface treatment. Hydrodynamic amplification factor increases with increase of filler volume content, its value depends on filler particles surface treatment. The decrease of hydrodynamic amplification factor during stretching correlates with the increase of viscoelastic strain. Taking into account the viscoelastic strain improves the description of the stress–strain response of filled rubber for loading–unloading process with the parameters obtained for active loading. © 2011 Wiley Periodicals, Inc. J Appl Polym Sci 123: 1621–1629, 2012

Key words: filled rubber; filler volume content; cluster; Klueppel–Schramm model

INTRODUCTION

The incorporation of small size particle fillers, such as carbon black or silica, to elastomeric networks ("filled rubber") produces a well known reinforcement effect[1]: the static shear or tensile modulus can be enhanced by nearly two orders of magnitude, and resistance to tear and abrasion is also noticeably improved. Reinforcement is thought to arise from the combination of the "hydrodynamic" effect, rubber-filler interactions, and long-range Van der Waals or short-range "contact" interactions between the filler particles. The interactions forces in filled rubber change under action of external loads: it results in reversible and irreversible changes of composite structure and properties, including deformational and strength properties. Depending on the load(s) application rates (quasistatic or dynamic loading) the irreversible changes of structure are reflected in Mullins[2] or Payne[3] effects, respectively.

The Mullins effect (called also stress or stretch-induced softening, or damage induced stress softening, or cyclic softening) is a reduction in stress of filled elastomers after the initial extension under repeated tensile strain. It is examined in constant strain rate tests under cyclic loading. The effect is mainly associated with a more compliant response of a prestretched material than that of the virgin material; the larger prior stretch ratio gives a greater softening of the response upon reloading. A qualitative review on the literature dedicated to the Mullins effect over past six decades was done in.[4]

The Payne effect is observed in the dynamic tests under cyclic loading conditions with small strain amplitudes and referred to a dependence of the viscoelastic storage modulus on the applied strain amplitude.

The Mullins and Payne effects have been the subject of numerous theories which can be more or less classified in two main types: (i) filler structure models, (ii) rubber-filler bonding and debonding models. The existence of two different pictures of the phenomena is directly related to the nanoscopic size of filler for which it is impossible to neglect either filler–filler interaction (with or without involvement of the matrix) or the rubber–filler interaction.

In the filler structure models, the filler–filler interactions are considered as predominant. Payne believed[3] that dependence of the moduli with strain is essentially determined by the agglomeration and de-agglomeration of the filler network. In the case of carbon black filled elastomers, above the percolation

Correspondence to: K. Aniskevich (a_klara@inbox.lv).
Contract grant sponsor: European Social Funds; contract grant number: project 2009/0209/1DP/1.1.1.2.0/09/APIA/VIAA/114.

threshold, when the filler particles come close together, the presence of filler network can be evidenced by electrical conductivity measurements. The rigidity of the structure depends on the rigidity of the filler–filler bonds. It is assumed that this filler network is damaged by application of a strain of sufficient magnitude that leads to the loss of rigidity. In case of silica filled elastomer, namely styrene-butadiene rubber (SBR), the breakdown of the filler aggregates with an increase of strain was successfully detected by transmission electron microscope (TEM).[5]

The second set of models assumes that the rubber–filler interactions are responsible for the Payne effect.[6] These models are based on the idea of adsorbed polymer at the filler surface (bound rubber) that displays a decreased molecular mobility and may act as supplementary crosslinks in the material. Then, under an increase of strain, a mechanism of adhesion and de-adhesion of polymer chain at the filler interface is proposed. The idea was confirmed by the use of electron spin resonance (ESR) technique to register the chain scissions of rubber molecules during stretching of silica filled SBR with filler particles treated by various coupling agents.[7] ESR results suggested that the degree of chain scission in silica filled SBR increased with increasing the mechanical energy applied to the samples during deformation.

Even in the adoption of the first type models the coupling of the filler to the matrix cannot be disregarded suggesting that filler–filler bonds in the filler network are probably made via an adsorbed layer of polymer onto the filler surface. Moreover, filler particles in aggregates can immobilize a nonvulcanized rubber since they prevent migration of this bound rubber into a surrounding solvent. The existence of entrapped rubber within the agglomerate was suggested by the TEM image analysis.[5] The amount seems to decrease with the decrease in agglomerate size. A part of the entrapped rubber might be realized when the filler network was broken by the strain.

In contrast to a rubbery state of the main part of matrix, the bound rubber in the interlayer may be in a glassy state. Above the percolation threshold, such layers can join creating glassy regions. If so, the mechanical behavior of filled rubbers should be typically viscoelastic exhibiting rate and temperature dependences, as well as dependence of the composite mechanical properties on treatment of the filler particle surface by coupling agent.

Taking into account the necessity of studying of at least two types of interactions in filled elastomers, a systematic experimental study of rubber both unfilled and filled with various filler volume contents, with and without treatment of filler particles surface is essential. This will give an insight into the mechanisms by which small size particles produce mechanical reinforcement in polymers above their glass transition temperature. To this purpose, the mechanical behavior of model composite under quasistatic loading up to failure, cyclic loading–unloading, and creep with different load levels was investigated. To evaluate the viscoelastic properties, the first part of the investigation was devoted to the analysis of creep and creep recovery test results.[8] This allowed us to describe the response to loading–unloading cycles with constant stretch ratio starting from the second cycle, i.e., after the Mullins effect was removed. In the present article, to find out the matrix and filler network parameters as functions of filler volume content and evaluate the changes of filler network structure during stretching of the material, the stress–stretch ratio curves up to failure are analyzed by using the mechanical model proposed in the literature. The effect of viscoelasticity on the response to first loading–unloading cycle, i.e., Mullins effect, is also considered.

MATERIALS AND TESTS

The material under investigation was SBR: unfilled and filled with silica particles without and with surface treatment by silane SI69 coupling agent. Filler volume contents for both series were approximately the same: $c = 0.0898$, 0.1411, and 0.208—for filler particles without surface treatment, and $c = 0.0886$, 0.1382, and 0.2018—for filler particles with surface treatment. Dumbbell test samples were cut from rubber sheets, whose thickness varied from 1.2 to 2 mm depending on material composition.

Uniaxial tension tests up to failure of the samples were performed on a universal testing machine Zwick 2.5, equipped with a load cell of 2.5 kN, at a constant crosshead speed of 5 mm/min, which corresponded to a nominal strain rate of 0.00333 s^{-1}. The samples were preloaded to 0.5 N to avoid bending.

Uniaxial cyclic tests: three loading–unloading cycles with increasing maximal stretch ratio of 0.25, 0.5 and 0.75 of ultimate were also performed at a constant crosshead speed of 50 mm/min, which corresponded to a nominal strain rate of 0.0333 s^{-1}.

Three to six samples of each composition were tested to get a repeatability of data. All tests were performed under laboratory conditions at an average temperature of 22°C.

The operative part of the samples, that is the part with maximum and uniform deformation, had a length of 20 mm and a width of 5 mm. This zone was delimited by white markers: two in the tension (axial) direction and two in the transversal (lateral) one. Markers in the thickness direction were also

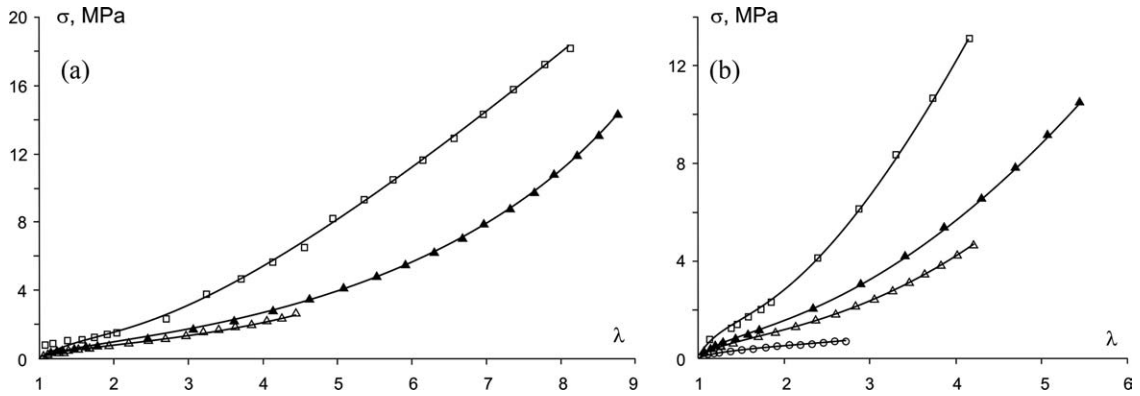

Figure 1 Stress–stretch ratio curves (up to failure) of rubber filled with various filler volume contents c for (a) untreated and (b) treated filler particles surface; dots are experimental data, lines are approximation by eqs. (3), (4), (6), and (7). For (a) $c = 0.0898$ (△), 0.141 (▲), 0.208 (□); for (b) $c = 0$ (○), 0.0886 (△), 0.1382 (▲), 0.2018 (□).

drawn on some samples. The displacements, which are proportional to the nominal strains, were registered by a high-resolution camera. Handling of photo images and evaluation of displacements was performed by using special software elaborated at the Institute of Polymer Mechanics developed in C++ on a platform.NET for Windows XP.[9] By using this noncontact method, it was possible to take into consideration displacements in operative part of the samples.

The lateral displacements in the width direction were measured for all samples. Measurements in the thickness direction were obtained for one sample of each composition and it was found for them that $\lambda_2 = \lambda_3$. Based on these data, the stretch field was assumed to be homogeneous in the operative part of each sample. Based on previous work,[10] it is assumed that the material is absolutely incompressible up to the stretch ratio equal to 4.5.

The experimental stress–stretch ratio curves of rubber both unfilled and filled are shown in Figure 1. It can be seen from the graphs that filling of the rubber noticeably raises its rigidity, strength, and stretch ratio at failure. Stress–stretch ratio curves of filled rubber are nonlinear: a convexity of each curve is replaced by concavity, revealing a point of inflection. The stress–stretch ratio curve of unfilled rubber is convex. Comparing the graphs in Figure 1(a,b), one can see that two series of composites: filled with particles without and with surface treatment exhibit different deformational and strength properties at the same filler volume content. For small filler volume content, $c \sim 0.09$, the former composite reveals smaller strength comparing to the latter. For larger filler volume contents, $c \sim 0.14$ and 0.2, the former composite reveals smaller rigidity but larger strength and considerably larger stretch ratio at failure than the latter.

As an example of cyclic loading–unloading test results, the stress–stretch ratio curves of filled rubber with filler volume contents $c \sim 0.2$ and 0.09 for untreated and treated surface of filler particles, respectively, are shown in Figure 2. The Mullins effect is obvious: a stretch-induced softening appears for stretch ratio lower or equal to the maximal stretch ratio ever attained. When the stretch ratio exceeds the maximal previously attained, the material stress–strain response returns on the same path as the monotonous uniaxial stress–strain response after a transition, which increases with the amount of stretch ratio. The degree of softening increases progressively with increasing maximal stretch ratio.

For both types of the composites: without and with filler particles surface treatment, the hysteresis loops decrease with decrease in the filler volume content and disappear for neat rubber.

THE KLUEPPEL–SCHRAMM MODEL OF ELASTICITY OF FILLER REINFORCED ELASTOMERS

The problem of obtaining a sufficiently general description of the stress–strain relation of rubber-like networks was investigated in numerous articles and was approached from both the phenomenological and molecular points of view. One of the surveys is presented in Ref. 11. The molecular point of view is preferable, as it allows description of the mechanical test results in terms of structure parameters, evaluation of the kinetics of their changes up to the composite failure, and determination of the rupture criteria.

Most attractive is a constitutive model of hyperelasticity and stress softening of filler reinforced polymer networks based on a molecular statistical theory of rubber elasticity[12] and a micro-mechanical concept of filler cluster failure in the deformed elastomer composites.[13,14] With its use, a good description of uniaxial stress–stretch ratio dependences of filler reinforced elastomeric networks both virgin and after prestrain is possible.[4,14–16]

The nonlinear elastic response of stretched polymer networks is described by a tube model of

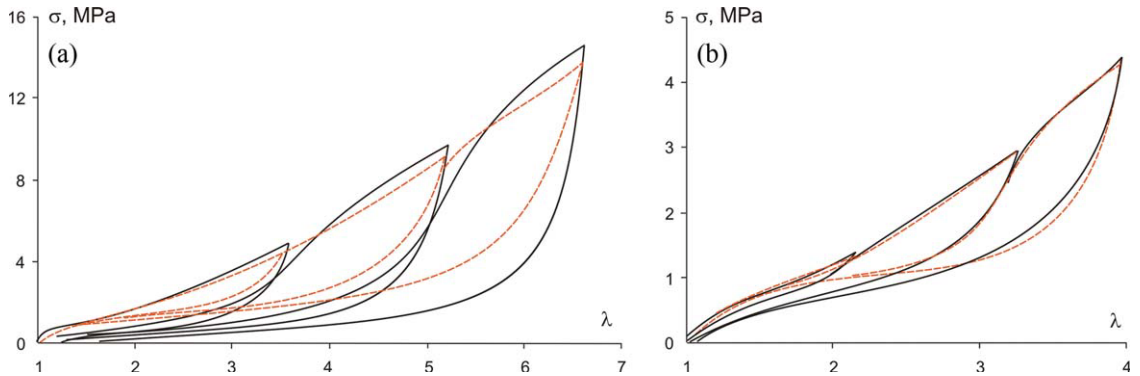

Figure 2 Stress as a function of stretch ratio for three loading–unloading cycles of rubber filled with surface untreated (a) and treated (b) particles for $c = 0.208$ and 0.1382, respectively; solid lines are experimental data, dotted lines are calculation by eqs. (3), (4), (6), and (7). [Color figure can be viewed in the online issue, which is available at wileyonlinelibrary.com.]

rubber elasticity.[12,13] In this model, it is assumed that the network chains in a highly entangled polymer network are heavily restricted in their fluctuations due to packing effects. These restrictions are described by virtual tubes around network chains. When the network elongates, the tubes deform less than affinely with a deformation exponent $v = 1/2$. It means that the tube radius r_μ in spatial direction μ of the main axes system depends on the stretch ratio λ_μ as follows

$$r_\mu = r_0 \lambda_\mu^v, \tag{1}$$

where r_0 is the tube radius in the nondeformed state.

The nonaffine tube model was originally derived for the case of Gaussian chain statistics.[12,13] For large strains, Klueppel and Schramm[14] took into account that the network chains have a finite length, and stress in the network becomes infinitely large, when the chains between two subsequent network junctions are stretched fully. Then, the free energy density of the extended, non-Gaussian tube model with nonaffine tube deformation is defined as

$$W_R = \frac{G_c}{2}\left\{\frac{\left(\sum_{\mu=1}^{3}\lambda_\mu^2 - 3\right)\left(1 - \frac{T_e}{n_e}\right)}{1 - \frac{T_e}{n_e}\left(\sum_{\mu=1}^{3}\lambda_\mu^2 - 3\right)} + \ln\left[1 - \frac{T_e}{n_e}\left(\sum_{\mu=1}^{3}\lambda_\mu^2 - 3\right)\right]\right\} + 2G_e\left(\sum_{\mu=1}^{3}\lambda_\mu^{-1} - 3\right). \tag{2}$$

The first bracket term of eq. (2) describes the constraints due to interchain junctions with an elastic modulus G_c proportional to the density of network junctions, i.e., crosslinks and trapped entanglements. The second addend considers the topological tube constraints, whereby G_e is proportional to the entanglement density of the rubber. The parenthetical expression in the first addend takes into account the finite chain extensibility.[13] For the limiting case, $\frac{n_e}{T_e} = \sum_{\mu=1}^{3}\lambda_\mu^2 - 3$, the free energy density, eq. (2), exhibits a singularity, which is reached when the chains between successive trapped entanglements are stretched fully. Here, n_e is the number of statistical chain segments between two subsequent entanglements and T_e is the trapping factor ($0 < T_e < 1$), which characterizes the portion of elastically active entanglements. T_e increases as the crosslink density increases, whereas n_e as term that is specific to polymer is to a great extent independent on crosslink density.

For uniaxial extension, $\mu = 1$, $\lambda_1 = \lambda$, of incompressible material $\lambda_2 = \lambda_3 = \lambda^{-1/2}$, the following relation for the nominal stress $\sigma = \frac{\partial W_R}{\partial \lambda}$ has been derived from eq. (2):

$$\sigma = G_c\left(\frac{1-d}{(1-dI_m)^2} - \frac{d}{1-dI_m}\right)\left(\lambda - \lambda^{-2}\right) + 2G_e\left(\lambda^{-1/2} - \lambda^{-2}\right), \tag{3}$$

where $I_m = \lambda^2 + \frac{2}{\lambda} - 3$, $d = T_e/n_e$.

Equation (3) applies to homogeneous unfilled rubber networks. It was shown to give a very good description of uniaxial stress–stretch ratio dependences up to high strains obtained for a variety of crosslink concentrations in natural rubber networks.

The presence in a soft highly deformable rubbery matrix of hard and much less deformable filler particles leads to a hydrodynamic effect: the required macroscopic (external) strain, ε, is achieved with the microscopic (internal) strain in the elastomeric matrix, ε_{int}, being higher than ε. The hydrodynamic reinforcement refers to a strain-amplification factor

$$X = \varepsilon_{int}/\varepsilon, \tag{4}$$

which describes the excessive strain of the polymer chains due to the presence of rigid filler particles. The internal (microscopic) stretch ratio is assumed to be amplified to $\lambda_{int} = 1 + \varepsilon_{int} = 1 + X\varepsilon$. This quantity

should be inserted for λ in eq. (3) to calculate the internal first strain invariant, or I_m, and the macroscopic stress observed at a macroscopic (external) strain ε. External stretch ratio is defined as $\lambda = 1 + \varepsilon$.

Filler particles are generally aggregated into clusters. The filler clusters result from an aggregation process in the rubber matrix subject to strong physical bonding between filler particles. Possible aggregation mechanisms are percolation or kinetical aggregation that both lead to a self-similar cluster with a disordered fractal-like structure. In case of high filler concentrations c with overlapping neighboring clusters, the following scaling law for hydrodynamic amplification factor was found by Huber and Vilgis[17]:

$$X = 1 + \text{const} \cdot \left(\frac{\xi}{a}\right)^{d_w - d_f} c^{\frac{2}{3-d_f}}. \quad (5)$$

Here ξ is the cluster size, a is the particle size, d_f is the fractal dimension, and d_w is the anomalous diffusion exponent of the clusters. Equation (5) shows that the strain amplification factor increases with filler concentration and cluster size according to a power law with an exponent that depends on the fractal structure of the clusters.

This result, eq. (5), was combined with a concept of stress-induced filler cluster breakdown, e.g., the model developed by Witten et al.[18] that considers the breakdown of self-similar filler clusters under lateral compression of the bulk polymer. With increasing strain of a virgin sample, a stress-induced breakdown of filler clusters takes place during which the size of the clusters decreases. This process is almost irreversible, since the gaps between broken filler clusters are filled up with elastomeric matrix during the material deformation. The elastomer is expected to be strongly bonded to the filler surface and, hence, it hinders reaggregation of the clusters when the stress relaxes during the unloading. The relevant strain-amplification factor X becomes a decreasing function of the external strain and is expressed as a function $X(L)$ of a scalar strain variable L:

$$X(L) = X_\infty + (X_0 - X_\infty)(1 + L)^{-\alpha}, \quad (6)$$

$$L = \left((1+\varepsilon)^2 + \frac{2}{(1+\varepsilon)}\right)^{1/2} - 1, \quad (7)$$

where parameters X_0 and X_∞ denote cluster sizes for zero and infinite strain limits, α is a rate of cluster breakdown.

An information on X for each filled rubber is obtained from stress–strain measurements. During the first stretching of a filler-reinforced network, the amplification factor decreases with strain in accordance with eqs. (6) and (7) and at maximal applied external stress, when L attains the value of L_{max}, it diminishes to $X(L_{max})$. On repeated stretching to ε_{max}, the uniaxial stress–stretch ratio dependence becomes stabilized for strains not exceeding ε_{max}, since the amplification factor $X(L_{max})$ has reached a constant value for all strains not exceeding the prestrain ε_{max} (i.e., for $\varepsilon < \varepsilon_{max}$, $L < L_{max}$). Thus, the dependency of the amplification factor on the strain is different for the first deformation of a virgin sample and for subsequent deformations, leading to the characteristic stress-softening.

Klueppel[16] measured uniaxial stress–stretch ratio dependences of filled styrene-butadiene and ethylene-propylene-diene terpolymer rubbers under various prestrains. By fitting the data by eqs. (3), (4), (6), and (7) the six parameters entering into these equations were determined. The fitting procedure was as follows: three parameters G_c, G_e, and d of eq. (3) and the value of X_{max} for each ε_{max} were obtained from unloading curves with maximal strain ε_{max}. By approximation of X_{max} as a function of ε_{max} with eqs. (6) and (7), the parameters X_0, X_∞, and α were obtained. The parameters were checked for stress–stretch ratio curve of virgin sample up to its failure. With increasing filler volume content, the parameters G_c, G_e, X_0, X_∞, and α showed a tendency to increase. Although in the limit of infinite stretch ratio, the theoretically expected minimal admissible value of X_∞ should not be lower than unity, for some systems, values lower than unity or even negative were found. However, in the experimental range of stretch ratio, the strain amplification factor X always remained reasonably higher than the physically realistic value of unity. It should be noted that obtaining the parameters from the unloading curves supposes that the effect of relaxation processes on deformational behavior is negligible.

APPROXIMATION PROCEDURE AND RESULTS

A procedure of the model parameters identification for the investigated materials was the following: (i) the experimental stress–stretch ratio curves of unfilled rubber were approximated by eq. (3) to obtain the parameters G_c, G_e, and d; (ii) these parameters were used as the initial values in subsequent obtaining of three parameters G_c, G_e, and d, characterizing elastic properties of rubber in the composite (filler reinforced rubber), and three parameters X_0, X_∞, and α, characterizing the filler cluster breakdown, by approximation of stress–stretch ratio curves of filled rubber for each filler volume content c with eqs. (3), (4), (6), and (7). To be not unreasonable, values $X_\infty - 1$, $X_0 - 1$, and α, as well as parameters G_c, G_e, and d, were positively defined.

For simultaneous estimation of three parameters G_c, G_e, and d of unfilled rubber and further six parameters G_c, G_e, d, X_0, X_∞, and α of filled rubber, at each c, a SIMPLEX algorithm with objective function

TABLE I
The Approximation Parameters of Stress–Stretch Ratio Curves of Unfilled and Filled Rubber by Eqs. (3), (4), (6), and (7)

		Filled					
	Unfilled	Surface treated filler particles			Surface untreated filler particles		
c	0	0.0886	0.1382	0.2018	0.0898	0.141	0.208
G_c (MPa)	0.19	0.067	0.162	0.387	0.0442	0.144	0.196
G_e (MPa)	0.232	0.912	1.03	1.3	0.672	0.631	1.02
$d \times 10^3$	8.79	4.08	1.36	0.571	3.72	0.931	0.431
X_0		13.9	20.8	31.5	13.9	19.6	34.1
$(X_\infty - 1) \times 10^3$		0.432	0.32	0.09461	0.405	0.436	0.114
α		1.65	1.41	1.34	1.65	1.26	1.28

in the form of the sum of the squared differences between experimental and predicted data was used. The advantage of this objective function is that it gives the optimal solution with the smallest possible residual.

The results of approximation of three experimental stress–stretch ratio curves for each c are shown in Figure 1. They are in a good agreement with experimental data. The approximation parameters are listed together in Table I.

DISCUSSION

To check the applicability of the above model, eqs. (3) and (4) along with eqs. (6) and (7), with parameters obtained from quasistatic loading tests up failure (Fig. 1), cyclic loading–unloading tests with increasing maximal stretch ratio (Fig. 2) were used. In accordance with the model, the hydrodynamic amplification factor $X(L)$ characterizes the filler cluster size in the rubber. Its irreversible change during active loading and constant value during unloading and repeated loading up to the stretch ratio, which does not exceed the level in previous cycle, was postulated in the model. The calculated hydrodynamic amplification factor as a function of stretch ratio $X(\lambda)$ for three considered loading–unloading cycles is shown in Figure 3 on the example of rubber filled with surface untreated particles for $c = 0.2$. The largest change of X is observed during the first cycle.

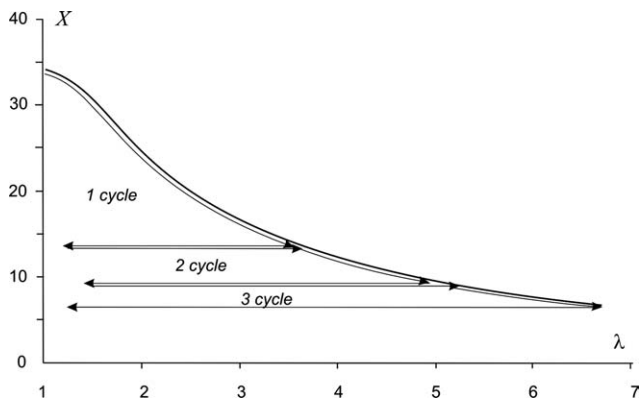

Figure 3 Calculated strain amplification factor as a function of stretch ratio for three loading–unloading cycles of rubber filled with surface untreated particles for $c = 0.208$.

Comparison of the calculated stress–stretch ratio curves with the experimental (Fig. 2) shows their similarity. But more careful consideration reveals some discrepancies. For all three cycles with increased maximal stretch ratio, the hysteresis loops and residual strains, i.e., strains at zero stresses, in calculated curves are smaller than in the experimental. The character of discrepancies is the same for all considered composites: with different c, for untreated and treated surface of filler particles. In the experimental unloading curves, the residual strain depends on the maximal stretch ratio in the cycle. The residual strain after loading–unloading cycle may be conditioned by relaxation processes and/or by a plastic flow in the structure, which were not accounted in the model.

Investigation of creep and creep recovery processes in the materials[8] showed that their

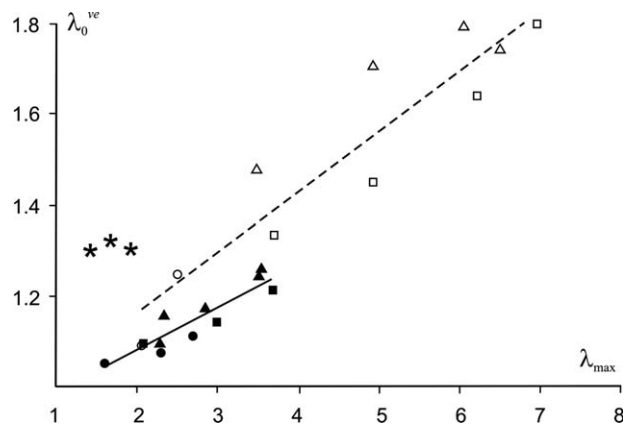

Figure 4 Instantaneous stretch ratio after stress is removed for creep recovery test of rubber unfilled (*) and filled with surface untreated (○, □, △) and treated (●, ■, ▲) particles for $c = 0.0898$ (○), 0.141 (□), 0.208 (△), and 0.0886 (●), 0.1382 (■), 0.2018 (▲).

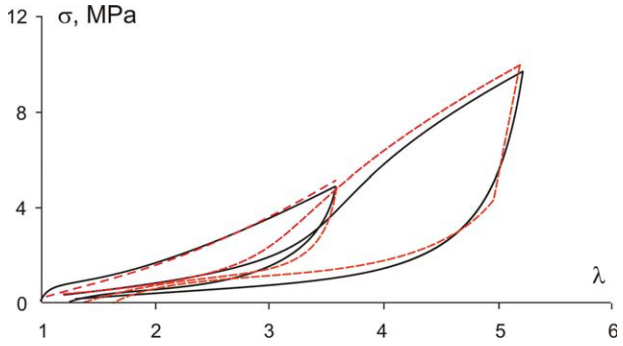

Figure 5 Stress as a function of stretch ratio for two loading–unloading cycles of rubber filled with surface untreated particles for $c = 0.208$; solid lines are experimental data, dotted lines are calculation by eqs. (3), (4), (6), and (7) taking into account viscoelastic strain, eq. (8). [Color figure can be viewed in the online issue, which is available at wileyonlinelibrary.com.]

deformational properties are viscoelastic. For creep recovery, the stretch ratio decreases with time t in accordance with the law

$$\begin{aligned} \lambda^{ve}(t) &= \lambda_0^{ve} t^{-k_1}, \quad \text{if } t \le t_s \\ \lambda^{ve}(t) &= \lambda_0^{ve} t_s^{k_2-k_1} t^{-k_2}, \quad \text{if } t > t_s \end{aligned}, \tag{8}$$

where λ_0^{ve} is instantaneous stretch ratio after the stress is removed, $t_s \sim 400$ s is characteristic time, k_1 and k_2 are rates of the process at different stages.

Both the λ_0^{ve} and rates k_1, k_2 increase with the increase of filler volume content c and maximal stretch ratio λ_{max}. As an example, the values of λ_0^{ve} for various λ_{max} and c are shown in Figure 4. They form two different lines: for rubber filled with surface untreated and treated particles, respectively. The values of λ_0^{ve} for neat rubber are outside of these lines. The same character was revealed for rates k_1 and k_2 as the functions of maximal stretch ratio λ_{max}. Thus, viscoelastic behavior of filled rubber differs from such of neat rubber and depends on surface treatment of filler particles. As surface treatment of filler particles changes the structure and properties of interlayer,[7] one can propose that the interlayer is responsible for viscoelastic properties of filled rubber.

Using eq. (8), the viscoelastic strain as the function of maximal stretch ratio and filler volume content was calculated and added to elastic strain in eqs. (3) and (7) to calculate the stress–strain response of filled rubber under cyclic loading–unloading. An example of the calculation result compared with the experimental data is shown in Figure 5. Taking into account the effect of viscoelasticity noticeably improves the calculation results: the hysteresis loops and residual strain enlarge. The effect is well shown for small stretch ratios.

Let's consider the model parameters with respect to composite structure. There are three parameters G_c, G_e, and d, characterizing rubber both unfilled and in the composite. The parameters G_c, G_e, and d determine an elastic modulus of rubber as

$$E = \frac{d\sigma}{d\lambda} \underset{\lambda \to 1}{\longrightarrow} 3[G_c(1-2d) + G_e]. \tag{9}$$

For parameter G_c, which is proportional to the density of network junctions, the dependence on filler volume content is nonmonotonic: small decrease changes by increase (Table I). The increase is larger for the rubber filled with surface treated particles compared to the rubber filled with surface untreated particles. This fact indicates that the surface treated filler particles act as additional crosslinks and the number of crosslinks increases with filler volume content. The parameter G_e, which is proportional to the entanglement density of the rubber, increases with c: practically linearly for rubber filled with surface treated particles, but more slowly for rubber filled with surface untreated particles. For the latter composite, the parameter d, which is proportional to the portion of elastically active entanglements and inversely to number of statistical chain segments between two subsequent entanglements, diminishes with c more rapidly. In accordance with eq. (9), the changes of parameters G_c, G_e, and d result in change of the elastic modulus E: it increases with c (Fig. 6). The increase is more essential in case of rubber filled with surface treated filler particles.

Considering the shear modulus G as the function of filler volume content for carbon black filled SBR,

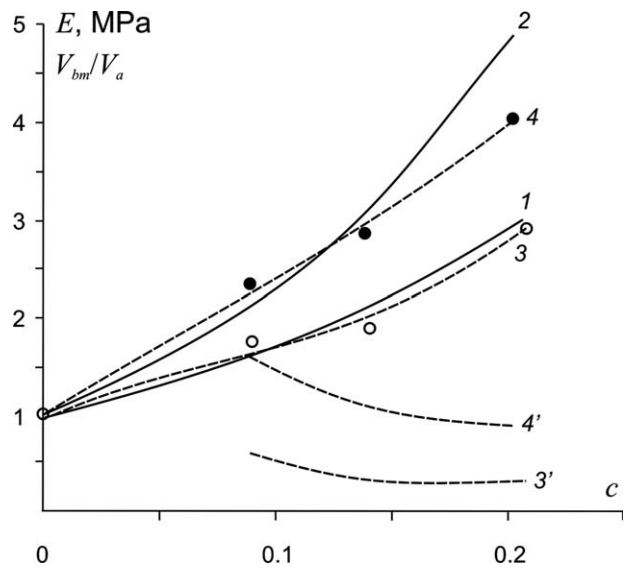

Figure 6 Elastic modulus of filled rubber as a function of filler volume content for filler particles with untreated (○) and treated (●) surface: dots are calculation by eq. (9) with approximated values of G_c, G_e, and d (Table I); lines are calculations by eq. (10) with $f = 1.44$, (1) 2.19, (2), and $f(c)$ (3,4) with V_{bm}/V_c as the function of c (3′, 4′).

Guido Raos[19] concluded that reinforcement can be qualitatively interpreted on the basis of simple hydrodynamic effect. He used the effective filler volume content $c_{\text{eff}} = fc$ in the modified Einstein formula, namely Guth–Gold expression:

$$\frac{G - G_0}{G_0} = 2.5c_{\text{eff}} + 14.1c_{\text{eff}}^2, \tag{10}$$

where G_0 is shear modulus of unfilled rubber.

The effectiveness factor f characterizes the rubber inside the aggregates,[20] the entrapped rubber, which is effectively shielded from stresses experienced by the bulk rubber. Thus, the amount of rubber bearing the stresses imposed upon the sample is reduced by the amount of entrapped rubber. It is further assumed that part of the entrapped rubber volume will be again elastically active under conditions of high strain.

In our case, a description of elastic modulus $\tilde{E} = \frac{E-E_0}{E_0}$, where E_0 is the elastic modulus of unfilled rubber, as a function of c using equation analogous to eq. (10) (lines 1 and 2 in Fig. 6) gave values of effectiveness factor 1.14 and 2.19 for rubber filled with particles without and with surface treatment, respectively. So, the effectiveness factor f depends on rubber–filler interaction. The aforesaid values of f are averages for all considered c. More precise description of $\tilde{E}(c)$ (lines 3 and 4 in Fig. 6) gives f as a function of c. In accordance with the definition, $f = 1 + \frac{V_{\text{bm}}}{V_a}$, where V_{bm} and V_a are volumes of entrapped rubber and filler, respectively. The calculated value of $\frac{V_{\text{bm}}}{V_a} = f - 1$ decreases with c (lines 3′ and 4′ in Fig. 6). It may be conditioned by the fact that in the composites with large c the filler particles contact with each other without rubber interlayer. For rubber filled with surface untreated particles, the relative volume content of entrapped rubber is relatively small. The applicability of eq. (10) type for description of the elastic modulus of composites considered in present work confirms that reinforcement effect for filled rubber can be interpreted on the basis of simple hydrodynamic effect. This is true for small stretch ratios.

In addition to elastic characteristics of the rubber, there are three parameters X_0, X_∞, and α, characterizing filler network in the composite during its stretching. As seen from Table I, parameter X_0, characterizing the initial size of filler cluster $\frac{\xi_0}{a}$ [eq. (5)], increases practically linearly with c: $\frac{2}{3-d_f} = 1$. Thus, a value of fractal dimension, $d_f = 1$, is obtained. Parameters X_∞, characterizing the minimal cluster size, and α, characterizing the rate of cluster destruction, decrease with c. Changes of X_∞ with c are very small, the parameter is practically equal to 1.

Using the filler network parameters X_0, X_∞, and α, a value of $\frac{\xi_0}{a}$ can be evaluated from eq. (5)

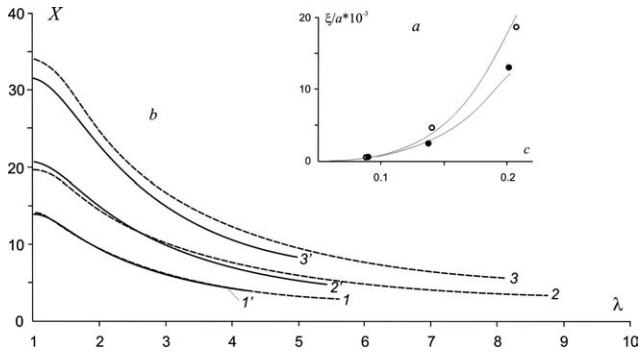

Figure 7 (a) Initial cluster size as a function of filler volume content for rubber filled with untreated (○) and treated (●) particles surface; (b) Strain amplification factor as a function of stretch ratio for rubber filled with various filler volume contents $c = 0.0886$, (1) 0.0898 (1′), 0.1382, (2) 0.1411 (2′), 0.208, (3) 0.2018 (3′) with (a) treated (1,2,3) and (b) untreated (1′, 2′, 3′) filler particles surfaces.

$$\ln\left(\frac{\xi_0}{a}\right) = \frac{1}{d_w - d_f} \ln\frac{X_0 - 1}{X_\infty - 1}, \tag{11}$$

where $d_w - d_f = \frac{\alpha}{\beta}$.

For $\beta = 1$, the initial size of filler cluster as a function of filler volume content is depicted in Figure 7(a). For small c, the initial size of filler cluster does not depend on filler particles surface treatment. With increase of c the dependence becomes noticeable: the initial sizes of filler cluster for rubber filled with surface treated particles are smaller then for untreated.

There is an apparent inconsistency in the results of initial cluster size $\frac{\xi_0}{a}$ and reinforcement effectiveness factor f for rubber filled with surface untreated and treated particles. To overcome it, one may conclude the following: in the latter composite, despite of smaller cluster size, more rubber is entrapped and strongly bounded with filler particles than in the former case. This is in line with the viscoelastic strain of filled rubber, which is smaller in the case of surface treated filler particles (Fig. 4).

In accordance with eqs. (6) and (7), dependence of hydrodynamic amplification factor X on stretch ratio is determined by parameters X_0, X_∞, and α. Their values change with filler volume content (Table I). So, functions $X(L)$ are different for various c. In Figure 7(b), X as a function of stretch ratio λ is plotted for various c to compare the functions $X(\lambda)$ with stress–stretch ratio curves in Figure 1(a,b). It may be seen from the graphs that X does not reach the value of X_∞ at the material failure; ultimate accessible values of X are different for various c. For small filler volume content, the hydrodynamic amplification factor does not depend on filler particles surface treatment. With increase of c, the dependence becomes noticeable: values of function $X(L)$, or $X(\lambda)$, for

rubber filled with surface untreated particles are larger than for treated. To compare the obtained data for hydrodynamic amplification factor as a function of strain, the dependencies $X(\lambda)$, corresponding to various c, can be normalized with their maximal value X_0. The procedure results in a common line for all considered composites: with various c, without and with filler particles surface treatment. Thus, the same process of filler cluster breaking in composites with various c came to light using the above considered identification of parameters of the model by approximation of the stress–stretch ratio curves up to material failure.

Comparing the graphs in Figure 7(b) with graphs in Figure 4, one can conclude that the process of cluster destruction is accompanied by the increase of time-dependent strain and the rates of relaxation process, underlying the creep recovery. As the interlayer is responsible for viscoelastic behavior, one may conclude that the interlayer in rubber filled with particles without surface treatment is more compliant and allows larger strains in comparison with the interlayer in rubber filled with surfaces treated particles.

CONCLUSIONS

Testing of silica filled SBR with various filler volume content without and with filler particles surface treatment under uniaxial tension, and analyzing the test results using the Klueppel–Schramm model of hyperelasticity and stress softening of filled rubber showed that:

- The model is applicable for description of the stress–stretch ratio curves during active loading process; description of unloading process with the same parameters has a systematic error, which can be diminished by accounting for the viscoelastic strains of the composites;
- Dependence of elastic modulus on filler volume content follows Guth–Gold equation, confirming the hydrodynamic nature of rubber reinforcement; the effectiveness factor increases with treatment of filler particles surface with coupling agent;
- Hydrodynamic amplification factor as a function of stretch ratio is dependent on filler volume content, as the initial cluster size and rate of cluster decay depend on filler volume content; a decrease of hydrodynamic amplification factor with the increase of stretch ratio correlate with the increase of viscoelastic strain;
- Dependence of hydrodynamic amplification factor on filler surface treatment was revealed for largest filler volume content.

References

1. Wolf, S., Wang, M.-J. In Carbon Black: Science and Technology, 2nd ed.; Donnet, J.-B., Bansal,R.C., Wang, M.-J., Eds.; Marcel Dekker: New York, 1993; Chapter 9.
2. Mullins, L.; Tobin, N. R. Rubber Chem Technol 1957, 30, 555.
3. Payne, A. R. J Appl Polym Sci 1962, 6, 57.
4. Diani, J.; Fayolle, B.; Gilormini, P. Eur Polym Mater 2009, 45, 601.
5. Yatsuyanagi, F.; Suzuki, N.; Ito, M.; Kaidou, H. Polymer 2001, 42, 9523.
6. Funt, J. M. Rubber Chem Technol 1987, 61, 842.
7. Suzuki, N.; Ito, M.; Yatsuyanagi, F. Polymer 2005, 46, 193.
8. Aniskevich, K.; Starkova, O.; Jansons, J.; Aniskevich, A. Mech Compos Mater 2010, 46, 4, 375.
9. Aniskevich, A.; Kalnroze, Z. Mater Technol Instrum 2008, 13, 105. [in Russian].
10. Starkova, O.; Aniskevich, A. Polym Test 2010, 29, 310.
11. Marckmann G.; Verron, E. Rubber Chem Technol 2006, 79, 5, 835.
12. Edwards, S. F.; Vilgis, T. A. Polymer 1986, 27, 483.
13. Kaliske, M.; Heinrich, G. Rubber Chem Technol 1999, 72, 602.
14. Klueppel, M.; Schramm, J. Macromol Theory Simul 2000, 9, 742.
15. Meissner, B.; Matejka, L. Polymer 2006, 47, 7997.
16. Klueppel, M. Macromolecules 1994, 27, 7179.
17. Huber, G.; Vilgis, T. A. Kautsch Gummi Kunstst 1999, 52, 102.
18. Witten, T. A.; Rubinstein, M.; Colby, R. H. J Phys II 1993, 3, 367.
19. Raos, G. Macromol Theory Simul 2003, 12, 17.
20. Heinrich, G.; Vilgis, T. A. Macromolecules 1993, 26, 1109.